



**HAL**  
open science

## New isomer in $^{96}\text{Y}$ marking the onset of deformation at $N = 57$

W. Iskra, B. Fornal, S. Leoni, G. Bocchi, A. Petrovici, C. Porzio, A. Blanc, G. de France, M. Jentschel, U. Köster, et al.

► **To cite this version:**

W. Iskra, B. Fornal, S. Leoni, G. Bocchi, A. Petrovici, et al.. New isomer in  $^{96}\text{Y}$  marking the onset of deformation at  $N = 57$ . *EPL - Europhysics Letters*, 2017, 117 (1), pp.12001. 10.1209/0295-5075/117/12001. in2p3-01481899

**HAL Id: in2p3-01481899**

**<https://hal.in2p3.fr/in2p3-01481899>**

Submitted on 24 Jan 2018

**HAL** is a multi-disciplinary open access archive for the deposit and dissemination of scientific research documents, whether they are published or not. The documents may come from teaching and research institutions in France or abroad, or from public or private research centers.

L'archive ouverte pluridisciplinaire **HAL**, est destinée au dépôt et à la diffusion de documents scientifiques de niveau recherche, publiés ou non, émanant des établissements d'enseignement et de recherche français ou étrangers, des laboratoires publics ou privés.

# New isomer in $^{96}\text{Y}$ marking the onset of deformation at $N = 57$

L. W. ISKRA<sup>1</sup>, B. FORNAL<sup>1</sup>, S. LEONI<sup>2,3</sup>, G. BOCCHI<sup>2,3</sup>, A. PETROVICI<sup>4</sup>, C. PORZIO<sup>2</sup>, A. BLANC<sup>5</sup>, G. DE FRANCE<sup>6</sup>, M. JENTSCHHEL<sup>5</sup>, U. KÖSTER<sup>5</sup>, P. MUTTI<sup>5</sup>, J.-M. RÉGIS<sup>7</sup>, G. SIMPSON<sup>8</sup>, T. SOLDNER<sup>5</sup>, C. A. UR<sup>9,10</sup>, W. URBAN<sup>11</sup>, D. BAZZACCO<sup>9</sup>, G. BENZONI<sup>3</sup>, S. BOTTONI<sup>2,3</sup>, A. BRUCE<sup>12</sup>, N. CIEPLICKA-ORYŃCZAK<sup>1,3</sup>, F. C. L. CRESPI<sup>2,3</sup>, L. M. FRAILE<sup>13</sup>, W. KORTEN<sup>14</sup>, T. KRÖLL<sup>15</sup>, S. LALKOVSKI<sup>12,16</sup>, N. MÁRGINEAN<sup>4</sup>, C. MICHELAGNOLI<sup>6</sup>, B. MELON<sup>17</sup>, D. MENGONI<sup>9,18</sup>, B. MILLION<sup>3</sup>, A. NANNINI<sup>17</sup>, D. NAPOLI<sup>19</sup>, ZS. PODOLYÁK<sup>12</sup>, P. H. REGAN<sup>12,20</sup> and B. SZPAK<sup>1</sup>

<sup>1</sup> *Institute of Nuclear Physics, PAN - PL-31-342 Kraków, Poland*

<sup>2</sup> *Dipartimento di Fisica, Università degli Studi di Milano - I-20133 Milano, Italy*

<sup>3</sup> *INFN, Sezione di Milano - via Celoria 16, I-20133, Milano, Italy*

<sup>4</sup> *Horia Hulubei National Institute of Physics and Nuclear Engineering - Bucharest, 077125, Romania*

<sup>5</sup> *ILL - 71 Avenue des Martyrs, F-38042 Grenoble CEDEX 9, France*

<sup>6</sup> *GANIL - BP 55027, F-14076 Caen CEDEX 5, France*

<sup>7</sup> *IKP, University of Cologne - Zùlpicher Str. 77, D-50937 Köln, Germany*

<sup>8</sup> *LPSC - 53 Avenue des Martyrs, F-38026 Grenoble, France*

<sup>9</sup> *INFN, Sezione di Padova - Padova, Italy*

<sup>10</sup> *ELI-NP - Magurele-Bucharest, Romania*

<sup>11</sup> *Faculty of Physics, University of Warsaw - ul. Pasteura 5, PL-02-093 Warsaw, Poland*

<sup>12</sup> *SCEM, University of Brighton - Lewes Road, Brighton BN2 4GJ, UK*

<sup>13</sup> *Grupo de Física Nuclear, Universidad Complutense, CEI Moncloa - 28040 Madrid, Spain*

<sup>14</sup> *CEA, Centre de Saclay, IRFU - F-91191 Gif-sur-Yvette, France*

<sup>15</sup> *Institut für Kernphysik, TU Darmstadt - Schlossgartenstrasse 9, D-64289 Darmstadt, Germany*

<sup>16</sup> *Faculty of Physics, University of Sofia - 5 James Bourchier Blvd, 1164 Sofia, Bulgaria*

<sup>17</sup> *INFN, Sezione di Firenze - Firenze, Italy*

<sup>18</sup> *Dipartimento di Fisica, Università degli Studi di Padova - I-35131 Padova, Italy*

<sup>19</sup> *INFN, Laboratori Nazionali di Legnaro - I-35020 Padova, Italy*

<sup>20</sup> *Acoustics and Ionizing Radiation Division, National Physical Laboratory Teddington, Middlesex, TW11 0LW, UK*

received 26 January 2017; accepted in final form 13 February 2017

published online 28 February 2017

PACS 23.20.Lv –  $\gamma$  transitions and level energies

PACS 25.85.Ec – Neutron-induced fission

PACS 21.60.-n – Nuclear structure models and methods

**Abstract** – The level scheme of  $^{96}\text{Y}$  was significantly extended and a new 201 ns isomer was located at 1655 keV excitation energy, with spin-parity assignment of  $5^{\pm}$  or  $6^{-}$ . The isomer decays to spherical low-spin structure by transitions with large hindrance and is fed by a short cascade which resembles the beginning of a rotational band. This is in analogy with the feeding and decay pattern of the  $4^{-}$  isomer in  $^{98}\text{Y}$ , here confirmed, by lifetime analysis, as a bandhead of a rotational structure with sizable deformation. It is suggested that the new isomer in  $^{96}\text{Y}$  arises from a shape change between deformed and spherical configurations, which indicates the appearance of deformation already at  $N = 57$  in the yttrium chain. The experimental findings for  $^{96}\text{Y}$  are strengthened by theoretical calculations based on the complex Excited Vampir model.

 Copyright © EPLA, 2017

The shape of a particular nucleus results from the interplay between the collective (macroscopic) and single-particle (microscopic) configurations and, therefore, it strongly depends on both the atomic number  $Z$  and the neutron number  $N$ . The neutron-rich nuclei around  $Z = 40$  and  $N = 60$  provide one of the best territories for the exploration of this sensitivity. Indeed, the sudden onset of the deformation observed for neutron-rich

nuclei with  $Z = 36\text{--}40$ , near  $N = 60$ , is considered the most dramatic shape change in the nuclear chart [1]. This shape transition can be interpreted in terms of the balance between the coexisting spherical and deformed configurations: while in the isotopes with  $N < 60$  the former is yrast, for  $N \geq 60$  the situation inverts with the deformed structure becoming yrast.

The coexistence of the spherical and deformed configurations and their inversion at  $N = 60$  has been clearly established in  $^{98\text{--}100}\text{Zr}$  [2,3],  $^{98\text{--}102}\text{Y}$  [4] and  $^{96\text{--}98}\text{Sr}$  [5] nuclei. In particular, in the chain of yttrium isotopes laser spectroscopic studies showed that: i) in the Y isotopes with neutron number from  $N = 50$  to  $N = 58$ , the ground and known isomeric states are nearly spherical; ii) in  $^{98}\text{Y}$  ( $N = 59$ ) the ground state is spherical while the  $T_{1/2} = 2.0\text{ s}$  metastable state exhibits rigid deformation —here, the spherical and deformed potential wells are almost degenerate; iii) beyond  $N = 59$ , and immediately at  $^{99}\text{Y}$  ( $N = 60$ ), the nuclear ground state is determined by a well-defined, deformed, potential minimum. A question arises as to whether the deformed structure described above, which shows up in yttrium nuclei only at  $N = 59$  and dominates the structure of more neutron-rich Y nuclei, can be present also in lighter Y isotopes.

To shed some light on this issue, we extended the information on the structure of the  $N = 57$  yttrium isotope, *i.e.*,  $^{96}\text{Y}$ , which was very poorly known prior to our work [6]. The new results include the identification of a new isomer at 1655 keV, with half-life  $T_{1/2} = 201(30)\text{ ns}$ . In this letter we will discuss its nature and the general structure of  $^{96}\text{Y}$ , in connection with beyond-mean-field calculations [7,8]. It will be shown that the structure above the isomeric state can be considered as a precursor of deformed configurations, appearing at lower excitation energies in heavier yttrium nuclei. This finding places  $^{96}\text{Y}$  at the onset of shape coexistence along the isotopic chain.

The  $\gamma$ -ray coincidence data on  $^{96}\text{Y}$  were obtained in the EXILL experimental campaign [9,10], making use of a highly efficient HPGe array, installed at the PF1B [11] cold-neutron facility at Institut Laue-Langevin (Grenoble, France). The ILL reactor is a continuous neutron source (with an in-pile flux up to  $1.5 \times 10^{15}$  neutrons  $\text{cm}^{-2} \text{ s}^{-1}$ ) and, after collimation to a halo-free pencil beam, the flux on target was  $10^8$  neutrons  $\text{cm}^{-2} \text{ s}^{-1}$ . Two detector setups were used, the first consisting of 8 EXOGAM clovers [12], 6 large coaxial detectors from GASP [13] and 2 ILL-Clover detectors, with a total photopeak efficiency of about 6% at 1.3 MeV. In the second setup, the GASP and ILL detectors were replaced by 16  $\text{LaBr}_3(\text{Ce})$  detectors, named FATIMA array [14], for lifetime measurements by fast-timing techniques [15–17].

The main part of the campaign (lasting two reactor cycles, each  $\approx 50$  days long) consisted of two long runs of neutron-induced fission on  $^{235}\text{U}$  and  $^{241}\text{Pu}$  targets. A digital, triggerless acquisition system (with time stamp intervals of 10 ns) allowed to study coincidences among  $\gamma$  transitions separated in time up to several tens of

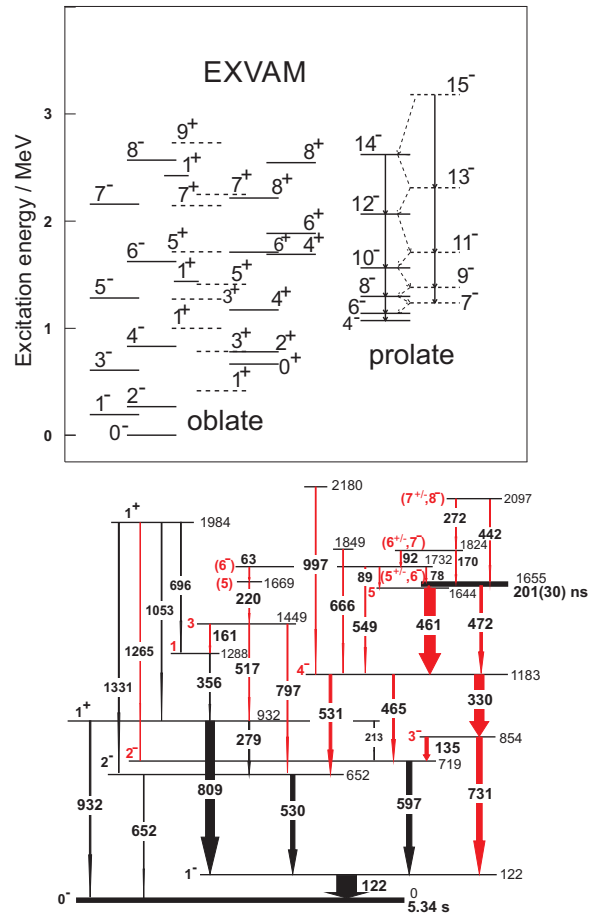


Fig. 1: (Color online) Experimental level scheme of  $^{96}\text{Y}$ : in black, transitions known prior to this work; in red, newly found transitions. The arrow widths reflect the observed transition intensities. Inset: theoretical spectrum obtained from the EXVAM model. The states are grouped according to the dominant oblate and prolate intrinsic quadrupole deformation.

microseconds [18,19]. For the purpose of investigating the excited structure of  $^{96}\text{Y}$ , with inclusion of the feeding and decay pattern of the newly found isomeric state, the data were sorted into two- and three-dimension histograms, by considering coincidences between i) *prompt*  $\gamma$ -rays —coincident (within 200 ns) with a fission event (defined by  $\gamma$ -ray multiplicity equal or larger than 4, within 200 ns) and ii) *delayed*  $\gamma$ -rays —emitted within a time interval of 100 ns–1  $\mu\text{s}$ , after the fission event and coincident between themselves within 200 ns.

Figure 1 shows the level scheme of  $^{96}\text{Y}$ , resulting from this work. Details of the analysis will be presented elsewhere [20] and [21], including the identification of the structure above the 9.6 s isomeric state, based on  $\gamma$ -ray coincidences with the fission partners. In this letter we concentrate, instead, on the structure around the newly found isomeric state, in the context of the appearance of collective bands in this otherwise spherical system.

Examples of coincidence spectra, partially documenting the identification of new  $\gamma$  transitions, are displayed

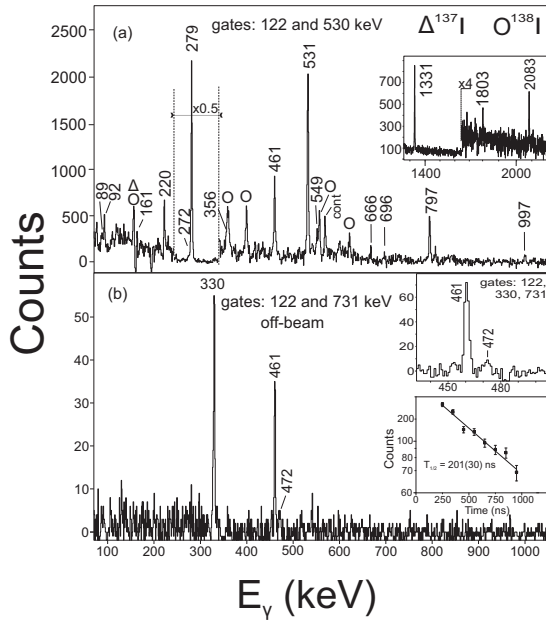


Fig. 2:  $\gamma$ -ray spectra of  $^{96}\text{Y}$  produced in neutron-induced fission on  $^{235}\text{U}$ . Panel (a): spectrum obtained requiring a double coincidence gate on 122 and 530 keV lines, prompt with fission (high-energy region in the inset). Transitions from the  $^{137,138}\text{I}$  fission partners are labelled. Panel (b): spectrum obtained requiring a double gate on the 122 and 731 keV transitions occurring in a time interval of 100 ns–1  $\mu$ s after the fission event. An additional gate on the 330 keV line was used to construct the spectrum in the inset. The decay curve of the new isomer is shown in the second inset (see text for details).

in fig. 2. The spectrum in panel (a) was obtained from the neutron-induced fission on  $^{235}\text{U}$ , by placing prompt double coincidence gates on the 122 and 530 keV lines, identified in the earlier  $\beta$ -decay study of  $^{96}\text{Sr}$  [22]. In addition to the previously known 279, 356, 696, and 1331 keV lines, new  $\gamma$ -rays clearly belonging to  $^{96}\text{Y}$  are displayed at 89, 92, 161, 220, 461, 531, 549, 666, 797, 997, 1803, and 2082 keV. Also, weak lines from the  $^{137,138}\text{I}$  fission partners are present in the spectrum. Figure 2(b), in which the spectrum gated on the delayed pair of transitions 122 and 731 keV is shown, demonstrates the existence of an isomeric state, which decays with emission of the 330, 461, and 472 keV transitions.

Further examination of mutual coincidences and the balance between prompt and off-prompt intensities of these three  $\gamma$ -rays, allowed us to locate a new isomeric state at 1655 keV excitation energy, which decays via the 472 keV and an unobserved 11 keV transitions with 13(3) and 87(7) % intensities, respectively (see fig. 1), and is fed from a well-established level at 1732 keV. By analyzing, as a function of time (with respect to the fission event), the intensities of the strong cascades depopulating the isomer, the half-life  $T_{1/2} = 201(30)$  ns has been deduced for the isomeric state, as shown in the inset of fig. 2(b).

The weak structure located above the isomer could be studied by prompt-delayed coincidences. Figures 3(a)

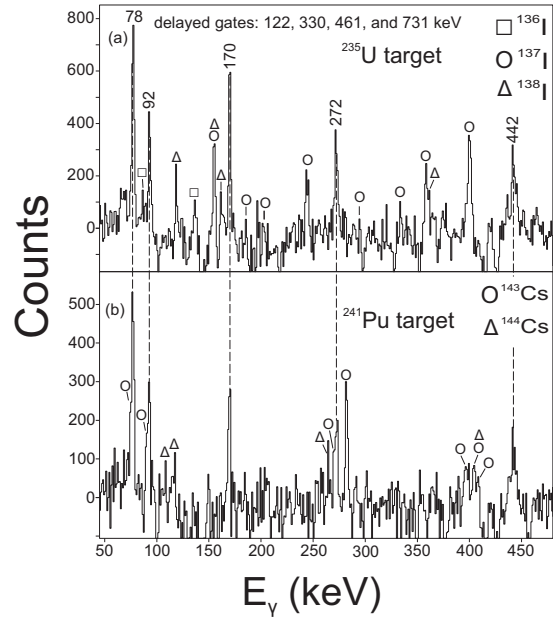


Fig. 3: Spectra of  $\gamma$ -rays prompt with fission events, obtained by summing double coincidence gates placed on all pairs of 122, 330, 461, and 731 keV delayed transitions. The panels refer to: (a) data taken with the  $^{235}\text{U}$  target; (b) with the  $^{241}\text{Pu}$  target. Transitions preceding the new 201 ns isomer are seen. The negative counts on both spectra result from the background subtraction.

and (b) show prompt spectra obtained from the  $^{235}\text{U}$  and  $^{241}\text{Pu}$  data, respectively, setting double gates on the four intense  $\gamma$  transitions depopulating the isomer. Both spectra show lines from the corresponding fission partners (iodine and cesium) and five transitions in common: the 78, 92, 170, 272, and 442 keV lines, which are, therefore, located above the 1655 keV isomeric state. The 92 and 272 keV lines have already been seen in the prompt spectrum of fig. 2(a), as they belong to cascades bypassing the isomer. Therefore, the additionally observed 78, 170, and 442 keV lines are feeding directly the 1655 keV isomeric state, as shown in fig. 1. No evidence was found for transitions feeding the  $(8^+)$  isomer ( $T_{1/2} = 9.6$  s) from the 1655 keV isomer and the levels above.

The spin-parity assignment for the 1655 keV isomer, as well as for a number of newly identified states, has been based on angular correlation analysis, decay branchings and the preferential feeding of yrast states in fission processes [23]. The angular correlations between  $\gamma$ -rays were studied using the EXOGAM clover detectors, applying the formalism described in refs. [24,25] and [26,27]. Figure 4 shows the analysis which allowed to establish the spin and parity of the 719, 854, 1183, and 1644 keV levels (fed by the isomer decay), which are relevant for the spin and parity assignment of the new 1655 keV isomeric state. All correlations are based on coincidences with the pure  $M1$  122 keV transition from the first excited  $1^-$  state to the ground state [22]. For the 854 keV level the  $3^-$  assignment is clear:  $\Delta I = 2$  for the 731 keV transition

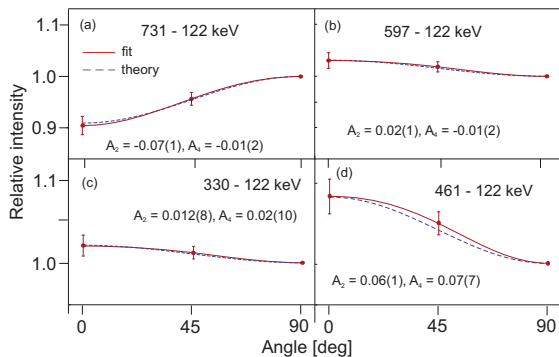


Fig. 4: (Color online) Selected examples of angular correlations in  $^{96}\text{Y}$ . The analysis was performed considering  $0^\circ$ ,  $45^\circ$ , and  $90^\circ$  (with  $135^\circ$  and  $180^\circ$  corresponding to  $45^\circ$  and  $0^\circ$ , respectively) average angles between the detectors, as done in refs. [26,27]. The energies of the  $\gamma$  transitions considered in each pair (see fig. 1) and the resulting  $A_2$  and  $A_4$  angular correlation coefficients are given.

(see fig. 4(a)), which is not isomeric. For the 1183 keV level, we assign  $4^-$ :  $\Delta I = 1$  for the 330 keV transition (fig. 4(c)) and no hindrance for the 531 keV transition feeding the  $2^-$  at 652 keV. For the 719 keV level, a  $2^-$  is given:  $\Delta I = 1$  for the 597 keV transition (fig. 4(b)) and no hindrance for the 465 keV transition. Finally, for the 1644 keV level,  $I = 5$  is assigned:  $\Delta I = 1$  for the 461 keV transition (fig. 4(d)).

Coming now to the new 1655 keV isomer, it decays to a  $I = 5$  state at 1644 keV by a 11 keV transition and by a much less intense 472 keV  $\gamma$ -ray to a  $4^-$  state at 1183 keV. This decay pattern restricts the spin assignment of the isomer to 5, 6 or 7. The  $I = 7$  assignment would imply the existence of unnaturally enhanced (by several orders of magnitude)  $M2$  or  $E2$  11 keV and  $M3$  or  $E3$  472 keV transitions. The assignment of  $6^+$  is very unlikely since there is no transition to the  $\beta$ -decaying ( $8^+$ ) isomer. The remaining possibilities are  $5^-$ ,  $5^+$  and  $6^-$ , the latter being also supported by the beyond-mean-field calculations discussed later. We note that the  $6^-$  assignment is also favoured by the preferential population of yrast states in fission reactions. The three previous possibilities imply very large hindrances for transitions deexciting the isomeric state: in the  $5^-$  or  $5^+$  case, the 472 keV  $M1$  or  $E1$  transition, respectively, to the  $4^-$  level at 1183 keV would be hindered by a factor of  $10^7$  or  $10^9$ . If  $6^-$  were adopted, the  $E2$  472 keV transition would be hindered by a factor of  $6 \times 10^4$ . Such hindered transitions are characteristic of  $K$ -forbidden or shape isomer decays.

A deeper insight into the problem of the observed hindrance may come from a comparison with the decay of the  $8.1 \mu\text{s}$   $4^-$  isomer in  $^{98}\text{Y}$ , located at 496 keV [28,29]. This isomer was suggested to be the bandhead of a rotational band which was identified on top of it. In earlier studies, the deformation of this band was tentatively extracted from the experimental  $\gamma$ -branching ratio of intraband transitions to be higher than 0.28 [30]. By using

Table 1: Results of the lifetime analysis of the states belonging to the deformed band in  $^{98}\text{Y}$ , above the  $4^-$  isomer. The electric quadrupole moment  $Q$  and deformation parameter  $\beta$  values are extracted by using the particle-rotor model [31] and the assumption of constant  $Q$ . See text and ref. [20] for details.

$I^\pi$	Energy (MeV)	$T_{1/2}$ (ps)	$B(E2) (I \rightarrow I - 2)$ (W.u.)	$Q$ (eb)	$\beta$
$5^-$	0.597	175(25)			
$6^-$	0.727	51(10)	45(14)	4.4(14)	0.49(16)
$7^-$	0.885	45(15)	37(14)	2.9(11)	0.32(12)
$8^-$	1.071	< 15	> 71.2	> 3.4	> 0.38

the EXILL data and by performing the lifetime analysis with fast-timing technique [15–17,20], we were able to obtain the values of the electric quadrupole moment  $Q$  of the band built on the  $4^-$  isomer in  $^{98}\text{Y}$ , which is strongly populated in our reactions. As shown in table 1, the deformation parameter  $\beta \approx 0.4$  was extracted, which is typical for rotational bands reported in Sr and Zr isotopes around  $N = 60$ .

This  $8.1 \mu\text{s}$   $4^-$  isomer in  $^{98}\text{Y}$  decays via two  $M1$  transitions into  $3^-$  and  $4^-$  spherical states at 446 and 375 keV, with a hindrance factor of the order of  $10^8$ . In addition, a limit on the existence of the  $E2$  transition into the  $2^-$  state at 171 keV, points to a large  $E2$  hindrance, higher than  $10^5$ . The new 201 ns isomer, located at 1655 keV, in  $^{96}\text{Y}$ , shows similar features in terms of hindrance of the decaying transitions, and arrangements in energy of the weak structure located above it (being 442 keV an  $E2$   $\gamma$ -ray feeding the isomer and 170 and 272 keV  $M1$  transitions, in a parallel branch). Therefore, we suggest that this may be considered the bandhead of a deformed structure, which progressively lowers its excitation energy when going from  $^{96}\text{Y}$  (energy 1655 keV), to  $^{98}\text{Y}$  (where it occurs at energy 496 keV), to 11 keV in  $^{100}\text{Y}$ , where it comes close to the ground state. This observation points to the onset of deformation already at  $N = 57$  in the yttrium isotopic chain.

From the theory point of view, the general features of the  $^{96}\text{Y}$  structure can be described by the beyond-mean-field approach, previously developed for neutron-rich nuclei in the  $A \simeq 100$  mass region [7,8], the *complex* Excited Vampir (EXVAM) variational model with symmetry projection before variation. A rather large model space above the  $^{40}\text{Ca}$  core built out of the  $1p_{1/2}$ ,  $1p_{3/2}$ ,  $0f_{5/2}$ ,  $0f_{7/2}$ ,  $2s_{1/2}$ ,  $1d_{3/2}$ ,  $1d_{5/2}$ ,  $0g_{7/2}$ ,  $0g_{9/2}$ , and  $0h_{11/2}$  oscillator orbits for both protons and neutrons was used. The effective two-body interaction was constructed from a nuclear matter  $G$ -matrix based on the Bonn CD potential. In order to enhance the pairing properties the  $G$ -matrix was modified by short-range (0.707 fm) Gaussians for the isospin  $T = 1$  and  $T = 0$  matrix elements. In addition, the isoscalar interaction was modified by monopole shifts for  $T = 0$  matrix elements of the form

$\langle 0g_{9/2}0f; IT = 0 | \hat{G} | 0g_{9/2}0f; IT = 0 \rangle$ . The Coulomb interaction between the valence protons was added.

The lowest positive- and negative-parity states up to spin 15 in  $^{96}\text{Y}$  were calculated. The final solutions, show a large variety of structures including states of pure oblate or prolate content, but also states with strong or weak oblate-prolate mixing.

The inset of fig. 1 shows the theoretical lowest bands of  $^{96}\text{Y}$ , grouped according to the presence of  $E2$  connections, with high  $B(E2)$  strengths. The calculations reproduce well the half-life of the low-lying states: for the lowest  $1^-$  state, the theoretical  $T_{1/2} = 120$  ps compares to the experimental value of 203 ps [6]; for the lowest  $2^-$  state, theory provides 1 ps while the experimental upper limit is 21 ps; for the lowest  $1^+$  state, the theoretical  $T_{1/2} = 22$  ps is close to the experimental upper limit of 21 ps.

By inspecting fig. 1, one observes that the lowest prolate deformed, negative-parity, band becomes yrast around 1 MeV of excitation energy. A striking feature is that the  $4^-$  state lies very close in energy with respect to the  $6^-$  prolate state. In addition, the negative-parity even-spin and odd-spin bands decaying to the  $6^-$  and  $7^-$  state, respectively, are connected by strong  $M1$  transitions. This resembles the beginning of the structure observed, in this work, on top of the 201 ns isomer. Consequently, the theoretical candidate for the newly identified isomer is the lowest prolate deformed  $6^-$  state. It is worthwhile to mention that calculations done for  $^{98}\text{Y}$ , involving only few EXVAM configurations, predict the existence of a similar pair of bands which could correspond to the deformed structure built on the  $4^-$  isomer.

In conclusion, in the present work the level scheme of  $^{96}\text{Y}$  was significantly extended and spin-parity for most of the identified states was assigned by the analysis of  $\gamma$ -ray angular correlations and the observed decay pattern. A new 201 ns isomer was located at 1655 keV excitation energy, with spin-parity assignment of  $5^\pm$  or  $6^-$ . The isomer decays to spherical low-spin structure and is fed by a short cascade which resembles the beginning of a rotational band. A large hindrance of the  $E2$  472 keV transition, deexciting the 201 ns isomeric state and feeding a  $4^-$  state, was observed. Similar features are found in the case of the  $4^-$  isomer in  $^{98}\text{Y}$ , at 496 keV. This isomer is fed by a rotational structure, for which we confirmed the size of the deformation ( $\beta \approx 0.4$ ) by lifetime analysis, and decays via very hindered  $M1$  transitions to spherical states. We propose that the isomerism of the bandhead of rotational structure in  $^{96}\text{Y}$  arises from a shape change from deformed to spherical configurations. The experimental findings for  $^{96}\text{Y}$  are strengthened by theoretical calculations based on the complex Excited Vampir model, which, among others, predicts the presence of a deformed  $6^-$  isomer, as a bandhead of a rotational prolate structure. The observation of rotational structures in  $^{96}\text{Y}$  points to an onset of deformation already at  $N = 57$ , which is in contrast with the earlier hypothesis of a sudden appearance of deformation only in the close proximity of  $N = 60$ .

This finding calls for further investigation of other  $N = 57$  isotones, at high excitation energies, in the  $A = 100$  mass region.

\*\*\*

The authors acknowledge the technical services of the ILL, LPSC and GANIL for supporting the EXILL campaign. The EXOGAM Collaboration and the INFN Legnaro are acknowledged for the loan of Ge detectors. This work was supported by the Italian Istituto Nazionale di Fisica Nucleare, by the Polish National Science Centre under Contract No. 2014/14/M/ST2/00738 and 2013/08/M/ST2/00257, by the UK Science and Technology Facilities Council and the UK National Measurement Office. Support from the German BMBF (contract No. 05P12RDNUP), the Spanish MINECO FPA2013-41267-P, NuPNET-FATIMA (PRI-PIMNUP-2011-1338) and the Romanian RO-FAIR F03/2016 is also acknowledged.

## REFERENCES

- [1] HEYDE K. and WOOD J. L., *Rev. Mod. Phys.*, **83** (2011) 1467.
- [2] URBAN W. *et al.*, *Nucl. Phys. A*, **689** (2001) 605.
- [3] HUA H. *et al.*, *Phys. Rev. C*, **69** (2004) 014317.
- [4] CHEAL B. *et al.*, *Phys. Lett. B*, **645** (2007) 133.
- [5] CLEMENT E. *et al.*, *Phys. Rev. Lett.*, **116** (2016) 022701.
- [6] NuDat - National Nuclear Data Center Brookhaven, <http://www.nndc.bnl.gov/nudat2/>.
- [7] PETROVICI A., *Phys. Rev. C*, **85** (2012) 034337.
- [8] JORDAN D. *et al.*, *Phys. Rev. C*, **87** (2013) 044318.
- [9] DE FRANCE G. *et al.*, *EPJ Web of Conferences*, **66** (2014) 02010.
- [10] JENTSCH M. *et al.*, *EXILL technical paper*, submitted to *JINST* (2015).
- [11] ABELE H., DUBBERS D., HASE H., KLEIN M., KNOPFLER A. *et al.*, *Nucl. Instrum. Methods Phys. Res. A*, **562** (2006) 407.
- [12] SIMPSON J., AZAIEZ F., DEFRANCE G., FOUAN J., GERL J., JULIN R., KORTEN W., NOLAN P. J., NYAKO B. M. *et al.*, *Acta Phys. Hung. New Ser.: Heavy Ion Phys.*, **11** (2000) 159.
- [13] ROSSI ALVAREZ C., *Nucl. Phys. News*, **3**, issue No. 3 (1993).
- [14] ROBERTS O. *et al.*, FATIMA Technical Design Report; ROBERTS O. *et al.*, *Nucl. Instrum. Methods Phys. Res. A*, **748** (2014) 91.
- [15] RÉGIS J.-M. *et al.*, *Nucl. Instrum. Methods Phys. Res. A*, **726** (2013) 191.
- [16] RÉGIS J.-M. *et al.*, *Nucl. Instrum. Methods Phys. Res. A*, **763** (2014) 210.
- [17] RÉGIS J.-M. *et al.*, *Phys. Rev. C*, **90** (2014) 067301.
- [18] MUTTI P. *et al.*, *Proceedings of the Advancement in Nuclear Instrumentation Measurement Methods and their Application (ANIMMA), 3rd International Conference, Marseille (IEEE, Marseille) 2013*, p. 1.
- [19] BOCCHI G. *et al.*, *Phys. Lett. B*, **760** (2016) 273.
- [20] ISKRA L. W. *et al.*, in preparation.

- [21] ISKRA L. W. *et al.*, to be published in *Acta Phys. Pol. B*.
- [22] JUNG G. *et al.*, *Nucl. Phys. A*, **352** (1981) 1.
- [23] AHMAD I. and PHILLIPS W. R., *Rep. Prog. Phys.*, **58** (1995) 1415.
- [24] MORINAGA H. and YAMAZAKI T., *In-beam Gamma-ray Spectroscopy* (North-Holland, Amsterdam) 1976.
- [25] FERGUSON A. J., *Angular Correlation Methods in Gamma-ray Spectroscopy* (North-Holland, Amsterdam) 1965.
- [26] CIEPLICKA-ORYNCZAK N. *et al.*, *Phys. Rev. C*, **93** (2016) 054302.
- [27] CIEPLICKA-ORYNCZAK N. *et al.*, *Phys. Rev. C*, **94** (2016) 014311.
- [28] BRANT S., LHERSONNEAU G. and SISTEMICH K., *Phys. Rev. C*, **69** (2004) 034327.
- [29] HWANG J. K. *et al.*, *Phys. Rev. C*, **58** (1998) 3252.
- [30] PINSTON J. A. *et al.*, *Phys. Rev. C*, **71** (2005) 064327.
- [31] RAGNARSSON I. and SEMMES P. B., *Hyperfine Interact.*, **43** (1988) 425.